Pharmaceutical Research, Vol. 23, No. 11, November 2006 (© 2006)
DOI: 10.1007/s11095-006-9102-6

Research Paper

Characterization of Hepatobiliary Transport Systems of a Novel α4β1/α4β7 Dual Antagonist, TR-14035

Minoru Tsuda-Tsukimoto,[1,3] Tomoji Maeda,[2] Takashi Iwanaga,[2] Toshiyuki Kume,[1] and Ikumi Tamai[2]

Received April 19, 2006; accepted June 26, 2006; published online September 13, 2006

Purpose. Our previous pharmacokinetic studies have demonstrated that TR-14035, a novel dual antagonist for α4β1/α4β7 integrin, selectively and strongly accumulated in the liver and was mainly excreted in bile as an unchanged drug. In the present study, we investigated the hepatobiliary transport system in detail.

Materials and Methods. Uptake by hepatocytes and organic anion transporting polypeptide (OATP)-expressing *Xenopus laevis* oocytes or Flp-In-293 cells was performed *in vitro.* Biliary excretion was investigated in *mdr1a/b*-knockout mice, *Bcrp*-knockout mice and *Mrp2*-defective Eisai hyperbilirubinemic rats (EHBRs).

Results. TR-14035 was taken up by rat and human hepatocytes by an apparently single saturable mechanism with K_m of 6.7 and 2.1 μM, respectively, and taurocholate and digoxin reduced this uptake. OATP1B1/OATP-C and OATP1B3/OATP8 expressed in oocytes mediated the TR-14035 uptake with K_m of 7.5 and 5.3 μM, respectively. OATP1B1*15, a genetic variant of OATP1B1, exhibited a decreased transport of TR-14035 compared with OATP1B1*1a. Biliary excretion and total body clearance of unchanged TR-14035 in EHBRs were significantly lower than those in normal rats, while there was no difference in the clearances between wild and *mdr1a/b*- or *Bcrp*-knockout mice.

Conclusion. These results indicate that OATP1B1 and OATP1B3 are at least partly responsible for the accumulation of TR-14035 into hepatocytes, and Mrp2 principally mediates the biliary excretion of TR-14035. Furthermore, genetic polymorphisms of *OATP1B1* may cause an interindividual variability in the pharmacokinetics of TR-14035.

KEY WORDS: genetic polymorphism; hepatobiliary transport; MRP2; OATP.

INTRODUCTION

The α4 integrins, α4β1 and α4β7, expressed on leukocytes, can bind to vascular cell adhesion molecule-1 and mucosal addressin cell adhesion molecule, respectively, localized on endothelial venules. This binding is critical for the firm adhesion of leukocytes to the endothelium, necessary for the subsequent transendothelial migration through the vessel wall (1,2). Therefore, α4β1 and α4β7 integrins are key regulators of physiologic and pathologic responses in inflammation and autoimmune diseases. Antagonists of α4β1 and α47 may have therapeutic applications in a number of diseases with an inflammatory component including inflammatory bowel disease, asthma, multiple sclerosis and rheumatoid arthritis.

TR-14035, *N*-(2,6-dichlorobenzoyl)-4-(2,6-dimethoxyphenyl)-L-phenylalanine (Fig. 1), is the first orally bioavailable chemical entity shown to be a potent and dual antagonist for α4β1/α4β7 integrin-mediated cell adhesion (3). Our previous study (4) has demonstrated that primary elimination routes of TR-14035 include the *O*-desmethylation of the dimethoxy-biphenyl ring and biliary excretion as an unchanged drug in the rat and dog. In human, *O*-desmethylation is also a principal route of TR-14035 metabolism, and cytochrome P450 2C9 (CYP2C9) is the primary enzyme responsible for the metabolism (5). In contrast, the mechanisms of hepatic uptake and biliary excretion of TR-14035 are still unclear. Therefore, when considering the pharmacokinetics of TR-14035, the present study focused on its hepatic uptake and biliary excretion.

[1] Exploratory DMPK, Exploratory Toxicology & DMPK Research Laboratories, Tanabe Seiyaku Co. Ltd., 2-2-50, Kawagishi, Toda, Saitama 335-8505, Japan.
[2] Faculty of Pharmaceutical Sciences, Tokyo University of Science, Chiba, Japan.
[3] To whom correspondence should be addressed. (e-mail: m-tsuda@tanabe.co.jp)

ABBREVIATIONS: AUC, area under the plasma concentration-time curve; BCRP, breast cancer resistance protein; CL_b, biliary excretion clearance; CL_r, urinary excretion clearance; CL_{tot}, total body clearance; CYP, cytochrome *P*450; EHBR, Eisai hyperbilirubinemic rat; FCCP, carbonyl cyanide-*p*-(trifluoromethoxy)-phenylhydrazone; K_m, Michaelis-Menten constant; k_{ns}, nonsaturable uptake clearance; KO, knockout; LC-MSD, liquid chromatography-mass spectrometric detection; LC-MS/MS, liquid chromatography-tandem mass spectrometry; MDR, multidrug resistance protein; MRP, multidrug resistance-associated protein; MRT, mean residence time; NTCP, sodium/taurocholate cotransporting polypeptide; OAT, organic anion transporter; OATP, organic anion transporting polypeptide; OCT, organic cation transporter; PAH, *p*-aminohippuric acid; PPB, plasma protein binding; SNP, single nucleotide polymorphism; TEA, tetraethylammonium; *Vd*, volume of distribution; V_{max}, maximum uptake rate.

0724-8741/06/1100-2646/0

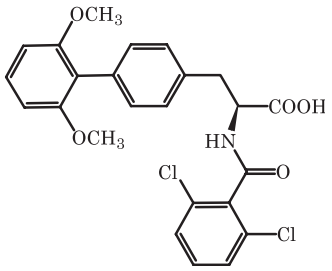

Fig. 1. Chemical structure of TR-14035.

At present, several uptake solute carriers are thought to be involved in the hepatic uptake of many kinds of drugs in human. Organic anion transporting polypeptide (OATP) 1B1 (OATP2/OATP-C/LST-1), OATP1B3 (OATP8/LST-2), organic anion transporter (OAT) 2, organic cation transporter (OCT) 1, and sodium/taurocholate cotransporting polypeptide (NTCP) are localized on the sinusoidal membrane of human hepatocytes (6–8). Among them, both OATP1B1 and 1B3 are selectively and predominantly expressed in the liver and have broad substrate specificities. The substrate specificities of OATP1B1 and 1B3 generally overlap each other, however, some disparities exist between them, for example, digoxin is a substrate of OATP1B3, but not OATP1B1 (6,8).

The biliary excretion of drugs and metabolites occurs predominantly by ATP-dependent drug efflux pumps that transfer substrates across the canalicular membrane into the bile. Multidrug resistance protein 1 (MDR1/ABCB1) and multidrug resistance-associated protein 2 (MRP2/ABCC2) are widely recognized efflux transporters and are responsible for the biliary excretion of a wide variety of compounds (8). Compared to the above pumps, breast cancer resistance protein (BCRP/ABCG2) is not well characterized, but mediates the biliary excretion of a variety of compounds (8,9).

In the present study, we investigated the hepatic uptake mechanism of TR-14035 utilizing rat and human hepatocytes and *Xenopus laevis* oocytes expressed with human OATP1B1 or 1B3, and the effect of single nucleotide polymorphism (SNP) of *OATP1B1* gene using OATP1B1*1a or 1B1*15 stably transfected cell lines. Transports of other OATP isoforms, OATP1A2 and 2B1, were also examined. In addition, we examined the biliary excretion of TR-14035 in *mdr1a/b*-knockout (KO) mice, *Bcrp*-KO mice and Eisai hyperbilirubinemic rats (EHBRs), whose *Mrp2* is hereditarily defective.

MATERIALS AND METHODS

Chemicals

TR-14035 was synthesized at Tanabe Seiyaku Co. and [^{14}C]TR-14035 (labelled uniformly on the benzene ring) was obtained from GE Healthcare Bio-Sciences (Piscataway, NJ). The specific radioactivity was 3.57 MBq/mg, and the radiochemical purity was greater than 97%, as determined by thin layer chromatography. TR-14085, *N*-(2,6-dichlorobenzoyl)-4-(2-ethoxy-6-methoxyphenyl)-L-phenylalanine, synthesized at Tanabe Research Laboratories was used as an internal standard for analysis. Digoxin, *p*-aminohippuric acid (PAH), taurocholate, rotenone and carbonyl cyanide-*p*-(trifluoromethoxy)-phenylhydrazone (FCCP) were purchased from Sigma-Aldrich (St. Louis, MO). Tetraethylammonium (TEA) was obtained from Wako Pure Chemical Industries (Osaka, Japan). [^{3}H]Estrone 3-sulfate and [^{3}H]estradiol 17β-glucuronide were purchased from PerkinElmer Life and Analytical Sciences (Boston, MA). [^{14}C]Inulin was purchased from American Radiolabeled Chemicals (St. Louis, MO). Cryopreserved human hepatocytes (Lot 63, 64 and 73) were purchased from In Vitro Technologies (Baltimore, MD). *X. laevis* oocytes expressing OATP1B1 (Lot 45 and 55) or OATP1B3 (Lot 69 and 75) were purchased from BD Gentest (Woburn, MA). All other reagents and solvents were of analytical grade and were commercially available.

Animals

Male Sprague–Dawley rats weighing 250 to 320 g were supplied from Charles River Japan (Yokohama, Japan) and used for hepatocyte uptake studies. Male FVB (wild), *mdr1 a/b* KO and *Bcrp* KO mice (19 to 24 g body weight) were purchased from Taconic Farms (Germantown, NY) and male Sprague–Dawley (normal) rats and EHBRs weighing 190 to 240 g were purchased from Japan SLC (Hamamatsu, Japan), and they were used for biliary excretion studies. Animals were acclimatized to management conditions for 7 days before commencement of treatment. All animal studies were reviewed and approved by the Animal Ethics Committee of Tanabe Seiyaku.

Biliary Excretion in Mice and Rats

For biliary excretion studies in mice and rats, a cannula (polyethylene tube, SP8 for mice and SP10 for rats; Natsume, Tokyo, Japan) was inserted into the bile duct of the anaesthetized animal. In the rat, after complete recovery from diethyl ether anesthesia, TR-14035 was administered intravenously at a dose of 3 mg/ml/kg, and the bile, urine and blood were collected at designated time intervals. In the mouse, TR-14035 was administered intravenously at a dose of 3 mg/4 ml/kg, and the bile and blood were collected at designated time intervals under pentobarbital anesthesia. Blood was centrifuged to separate plasma, and all the samples were stored at −20 °C until analysis by LC-MSD (Agilent Technologies, Palo Alto, CA).

Aliquots of the plasma, bile and urine samples were added to 0.5 ml of 1 M KH_2PO_4 and 10 μl of TR-14085 (2 μg/ml in acetonitrile) as an internal standard, and extraction was carried out using 5 ml of diethyl ether. After evaporation to dryness under nitrogen gas, the residue was reconstituted in 10% (v/v) acetonitrile, and injected on LC-MSD. The LC-MSD system consisted of an Agilent 1100 autosampler and an Agilent 1100 binary pump fitted with a Symmetry C18 column (3.5-μm particle size, 2.1 mm × 150 mm; Waters, Milford, MA). The column temperature was maintained at 45°C. The mobile phase consisted of 0.1% (v/v) acetic acid aqueous solution (solvent A) and acetonitrile (solvent B) and delivered at a flow rate of 0.25 ml/min. The initial mobile phase consisted of 20% of solvent B, which was increased linearly to 80% over 4 min, and maintained for 10 min. The following MSD conditions were applied: drying gas flow, 12 l/min; nebulizer pressure, 50 psi; capillary voltage, 3,500 V;

drying gas temperature, 300°C; negative selected-ion monitoring mode; and fragmentor voltage, 150 V. TR-14035 concentrations were determined by monitoring ions at m/z 472 (for TR-14035) and m/z 486 (for internal standard).

Binding to Plasma Proteins

The binding of TR-14035 to mouse and rat plasma proteins was determined by the ultrafiltration method. Following a 5-min incubation of blank plasma spiked with TR-14035 (final 1 μg/ml) at 37°C, aliquots of the plasma sample were immediately transferred to centrifuge tubes (Centrifree YM-30; Millipore, Bedford, MA). The tubes were centrifuged at 37°C and the resulting ultrafiltrates were collected. Each aliquot of the original plasma sample and its ultrafiltrate was analyzed by LC-MSD as described above.

Uptake by Rat and Human Hepatocytes

Rat hepatocytes isolated by the procedure described by Baur *et al*. (10) were suspended (2×10^6 cells/ml) on ice in Krebs–Henseleit buffer supplemented with 12.5 mM HEPES (pH 7.4). Rat hepatocyte viabilities for each experiment were routinely checked by the trypan blue exclusion test, and were greater than 85%. Cryopreserved human hepatocytes were stored in liquid N_2 until use. Thawing was achieved by gently shaking the vials of cryopreserved hepatocytes in a 37°C water bath. As soon as all contents had been thawed, the vials were immediately placed on ice and diluted with Krebs–Henseleit buffer supplemented with 12.5 mM HEPES (pH 7.4) at 4°C. After dilution, the human hepatocyte suspension was washed by centrifugation at $50 \times g$ for 5 min and resuspended in the same buffer (2×10^6 cells/ml). Viabilities of cryopreserved human hepatocytes used were in the range of 74 to 84%. All experiments were completed within 2 h after cell preparation, at which time viability had not changed appreciably.

The uptake experiments were performed as described previously (11). Briefly, uptake of [^{14}C]TR-14035 was initiated by the addition of ligand solution into the hepatocyte suspension (final 1×10^6 cells/ml) preincubated at 37°C for 3 min. At a designated time, the reaction was terminated by separation of hepatocytes from the incubation medium by a centrifugal filtration method (12). Each cell pellet was solubilized with alkaline solution and neutralized with HCl. The radioactivities in the medium and cells were determined using a liquid scintillation spectrophotometer (2500 TR; PerkinElmer Life Sciences, Boston, MA), after addition of scintillation cocktail (Clear-sol I; Nacalai Tesque, Kyoto, Japan). To minimize the contribution of nonspecific binding to the cell surface, the initial uptake velocity of TR-14035 was calculated using a linear regression of points between 20 and 60 s. For inhibition studies, various chemical inhibitors were added to the hepatocyte suspension 3 min (FCCP and rotenone: 15 min) before the addition of [^{14}C]TR-14035 solution to examine their effect.

Uptake by Oocytes Expressed with OATPs

OATP1B1- or 1B3-expressing and uninjected oocytes arrived at our institute 6 days after cRNA injection, and were immediately devoted to following uptake studies. OATP1B1 and 1B3 activities for each lot were routinely checked by the uptake of [^{3}H]estrone 3-sulfate (2 μM) and [^{3}H]estradiol 17β-glucuronide (2 μM), typical substrates of OATP1B1 and 1B3, respectively. Uptake activities in OATP1B1 and uninjected oocytes were 0.622 and 0.146 pmol/oocyte/h, respectively (Lot 45), and 0.566 and 0.105 pmol/oocyte/h, respectively (Lot 55). Uptake activities in OATP1B3 and uninjected oocytes were 0.578 and 0.102 pmol/oocyte/h, respectively (Lot 69), and 0.352 and 0.076 pmol/oocyte/h, respectively (Lot 75). cDNAs of *OATP1A2* and *2B1* were subcloned into pcDNA3.1 and pcDNA3 vectors, respectively and synthesized their cRNA *in vitro* using T7 RNA polymerase as described previously (13). Following cRNA injected oocytes were cultured for 3 days, the oocytes were used for uptake experiments. Uptake activities of [^{3}H] estrone 3-sulfate (12 nM) in OATP1A2, 2B1 and control oocytes were 1.64, 39.5 and 3.88 fmol/oocyte/h, respectively. The uptake experiment was performed as described previously (14) with minor modifications. In brief, uptake of TR-14035 was measured at room temperature in sodium buffer containing 100 mM NaCl, 2 mM KCl, 1 mM $MgCl_2$, 1 mM $CaCl_2$, and 10 mM HEPES (pH 7.4). The uptake was initiated by replacing sodium buffer with that containing TR-14035 and was terminated by the addition of ice-cold sodium buffer at a designated time. Oocytes were washed five times with ice-cold sodium buffer, individually transferred into a tube, and stored at −20°C until analysis by LC-MS/MS as described below.

Generation of Stable Cell Lines Overexpressing OATP1B1*1a and OATP1B1*15

cDNA of *OATP1B1*1a* or *OATP1B1*15* in the expression vector pcDNA3 (Invitrogen, Carlsbad, CA) was digested with Kpn I and ligated into the same site of pcDNA5/FRT (Invitrogen). The resulting vectors containing OATP1B1*1a, OATP1B1*15 or pcDNA5/FRT (termed mock) were co-transfected with pOG44 into a Flp-In-293 host cell line (Invitrogen) using calcium-phosphate precipitate formation (15). Stable integrants were selected in Dulbecco's modified Eagle's medium containing 10% fetal bovine serum, 1×10^5 U/l penicillin G, 100 mg/l streptomycin and 200 mg/l hygromycin B (Invitrogen) for about 2 weeks.

Uptake by Cells Expressed with OATP1B1*1a and OATP1B1*15

The uptake experiments were performed as described previously (16). Briefly, the cells overexpressing OATP1B1*1a, OATP1B1*15 and mock were harvested and suspended in transport medium containing 125 mM NaCl, 3 mM KCl, 5.6 mM D-glucose, 1.2 mM $CaCl_2$, 1.2 mM KH_2PO_4, 1.2 mM $MgSO_4$, and 25 mM HEPES (pH 7.4). Uptake was initiated by the addition of [^{3}H]estrone 3-sulfate (final 8.7 nM) or TR-14035 (final 2.5 μM) into the cell suspension preincubated at 25°C for 10 min. At a designated time, the cells were separated from the medium by centrifugal filtration. In the uptake of [^{3}H]estrone 3-sulfate, each cell pellet was solubilized and associated radioactivity was determined. In the uptake of TR-14035, each cell pellet was suspended with 250 mM sucrose and stored at −20°C until

analysis by LC-MS/MS as described below. The uptake rates of [^{3}H]estrone 3-sulfate and TR-14035 were corrected for the adherent volume calculated from the [^{14}C]inulin uptake.

LC-MS/MS Analysis

Samples from the TR-14035 uptake study by oocytes and Flp-In-293 cells were analyzed by an HP 1100 LC system (Agilent Technologies, Palo Alto, CA) coupled to an API3000 triple quadrupole mass spectrometer (Applied Biosystems/MDS Sciex, Foster City, CA). One hundred microliters of acetonitrile/methanol (1:1, v/v) including TR-14085 as an internal standard were added to each tube including one oocyte, and the tube was sonicated for 30 s and then centrifuged at 10,000 × *g* for 10 min. The resultant supernatant was removed and evaporated to dryness under nitrogen gas. The residue was reconstituted in 10% (v/v) acetonitrile, and injected on LC-MS/MS. Forty microliters of Flp-In-293 cell suspensions were added to 50 μl of acetonitrile/methanol (1:1, v/v) and 10 μl of TR-14085 in acetonitrile as an internal standard, and were centrifuged at 10,000 × *g* for 5 min. The resultant supernatants were injected on LC-MS/MS. Chromatography was carried out on an Inertsil ODS-3 column (5-μm particle size, 3.0 × 20 mm; GL Sciences, Tokyo, Japan). The mobile phase consisted of 0.1% formic acid aqueous solution (solvent C) and acetonitrile (solvent D) and delivered at a flow rate of 0.5 ml/min. The initial mobile phase consisted of 5% of solvent D held for the first 0.5 min, which was linearly increased to 95% of solvent D at 2 min, and was reverted back to initial conditions at 2.5 min for column re-equilibration. Mass spectrometer was operated in negative ion electrospray mode, and analyte detection was performed using multiple reaction monitoring. Electrospray voltage and source temperature were −4200 V and 500°C, respectively. Nitrogen was used as the collision gas, and collision energy was set at −60 and −30 eV for TR-14035 and TR-14085, respectively. The mass transitions for monitoring were m/z 472→212 and 486→297 for TR-14035 and TR-14085, respectively.

Kinetic Analysis

The kinetic parameters for the uptake of TR-14035 by hepatocytes were obtained using the following equation: $v = V_{max} \times S/(K_m+S)+k_{ns} \times S$, where v is the uptake rate of substrate (pmole/10^6 cells/min), S is the substrate concentration in the incubation medium (μM), K_m is the Michaelis-Menten constant (μM), V_{max} is the maximum uptake rate (pmol/10^6 cells/min), and k_{ns} is the apparently nonsaturable uptake clearance (μl/10^6 cells/min). The kinetic parameters for the uptake of TR-14035 in oocytes were estimated from the following equation: $v = V_{max} \times S/(K_m+S)$, where v is the uptake rate of substrate (pmol/oocyte/h) which is obtained by subtracting the transport velocity in uninjected oocytes from that in OATP1B1- or 1B3-expressing oocytes, S is the substrate concentration in the incubation medium (μM), K_m is the Michaelis-Menten constant (μM), and V_{max} is the maximum OATP1B1- or 1B3-mediated uptake rate (pmol/oocyte/h). To calculate the kinetic parameters, the above equations were fitted to uptake data sets by an iterative nonlinear least squares method using MULTI program (17). The input data were weighted as the reciprocal of the observed values, and the Damping Gauss-Newton Method algorithm was used for fitting.

The pharmacokinetic parameters were calculated by following non-compartment methods. The area under the plasma concentration-time curve (AUC) and the area under the first moment of plasma concentration-time curve (AUMC) were calculated by the trapezoidal method. Total body clearance (CL_{tot}), mean residence time (MRT) and volume of distribution (Vd) were calculated from Dose/AUC, AUMC/AUC and $CL_{tot} \times$ MRT, respectively. Biliary excretion clearance (CL_b) and urinary excretion clearance (CL_r) were calculated by the cumulative amount of unchanged TR-14035 excreted into the bile and urine, respectively, divided by AUC. Percentage of TR-14035 bound in the plasma protein was calculated by $(C_p-C_f)/C_p \times 100$, where C_p and C_f are the concentration in the plasma and filtrate, respectively.

Statistical Analysis

All statistical tests were performed using the Prism software package (version 3.02, GraphPad, San Diego, CA). Statistical differences in the rat biliary excretion study were calculated by a two-sided unpaired Student's *t*-test. Statistical analyses in the mouse biliary excretion study were performed using one-way ANOVA, followed by Dunnett's test to compare *mdr1a/b* KO or *Bcrp* KO mice with wild mice. The criterion for statistical significance was $p < 0.05$.

RESULTS

Uptake of TR-14035 by Rat and Human Hepatocytes

As shown in Fig. 2, [^{14}C]TR-14035 at 0.5 μM was taken up by the isolated rat and cryopreserved human hepatocytes in a time-dependent manner. Replacement of sodium with

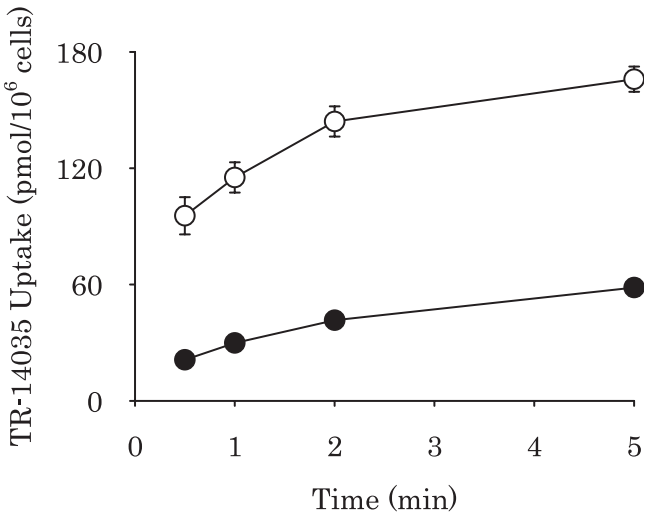

Fig. 2. Time course of [^{14}C]TR-14035 uptake by rat: *open circles* (○) and human: *closed circles* (●) hepatocytes. Hepatocytes (1 × 10^6 cells/ml) were incubated with 0.5 μM [^{14}C]TR-14035 at 37°C for 0.5, 1, 2 and 5 min. Each point represents the mean ± S.E. of three independent lots in duplicate.

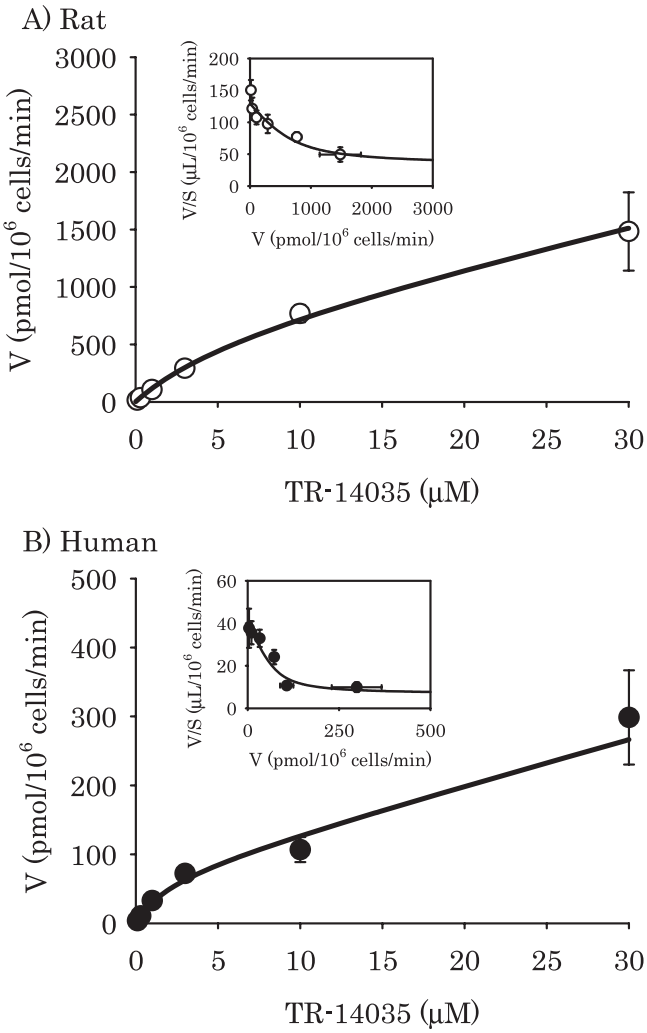

Fig. 3. Concentration-dependence of [^{14}C]TR-14035 uptake by rat (A, *open circles* (○)) and human (B, *closed circles* (●)) hepatocytes. Hepatocytes (1×10^6 cells/ml) were incubated with [^{14}C]TR-14035 at 37°C for 20 and 60 s. Initial uptake velocity (V) was calculated using a linear regression of points between 20 and 60 s. *Inset*, Eadie–Hofstee plot for the data. *Solid lines* represent the fitted curves obtained by non-linear regression analysis. Each point represents the mean ± S.E. of three independent lots in duplicate.

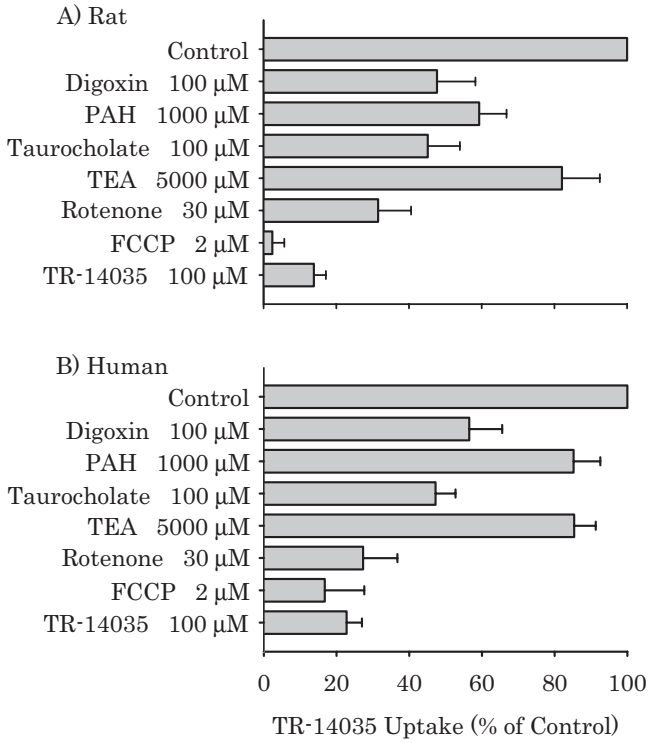

Fig. 4. Effect of typical inhibitors on [^{14}C]TR-14035 uptake by rat (A) and human (B) hepatocytes. Each inhibitor was incubated with hepatocytes (1×10^6 cells/ml) including 0.5 μM [^{14}C]TR-14035 at 37°C. Each *bar* represents the mean ± S.E. of three independent lots in duplicate.

choline in the incubation medium had no effect on uptake of [^{14}C]TR-14035 in both hepatocytes (data not shown). Figure 3 shows the effect of substrate concentration on initial uptake rate of [^{14}C]TR-14035 by rat and human hepatocytes. The initial uptake rate by the hepatocytes increased in a concentration-dependent manner, and Eadie-Hofstee plot showed apparently one saturable component with an apparently nonsaturable component in the TR-14035 uptake. The uptake kinetic parameters were estimated by the equation described in the Materials and Methods section and the estimated kinetic parameters are shown in Table I. The apparent K_m value of [^{14}C]TR-14035 uptake in human hepatocytes was 3.31 ± 1.42 μM, which was approximately half of that in rat hepatocytes. In contrast, the intrinsic uptake clearance in human hepatocytes, calculated by V_{max}/K_m, was 35.0 μl/10^6 cells/min, was approximately one-third of rat intrinsic clearance due to an approximately five times higher V_{max} value in rat hepatocytes.

The initial uptake of [^{14}C]TR-14035 at 0.5 μM by rat and human hepatocytes decreased in the presence of ATP depletors, rotenone and FCCP (Fig. 4). Taurocholate, a bile acid, and digoxin, a substrate of rat Oatp1a4 and human OATP1B3, inhibited [^{14}C]TR-14035 uptake by both hepatocytes. PAH, a typical substrate for OATs, also inhibited the uptake by rat hepatocytes, but not by human hepatocytes. In

Table I. Kinetic Parameters of TR-14035 Uptake in Rat and Human Hepatocytes

Species	K_m	V_{max}	V_{max}/K_m	k_{ns}
	(μM)	(pmol/10^6 cells/min)	(μl/10^6 cells/min)	(μl/10^6 cells/min)
Rat	6.33 ± 3.09	619 ± 227	97.8	33.5 ± 8.6
Human	3.31 ± 1.42	116 ± 58	35.0	3.85 ± 3.61

Data shown in Fig. 3 were used to determine these parameters calculated by nonlinear regression analysis. Each value represents the mean ± S.D. of the parameter estimate generated by the MULTI program.

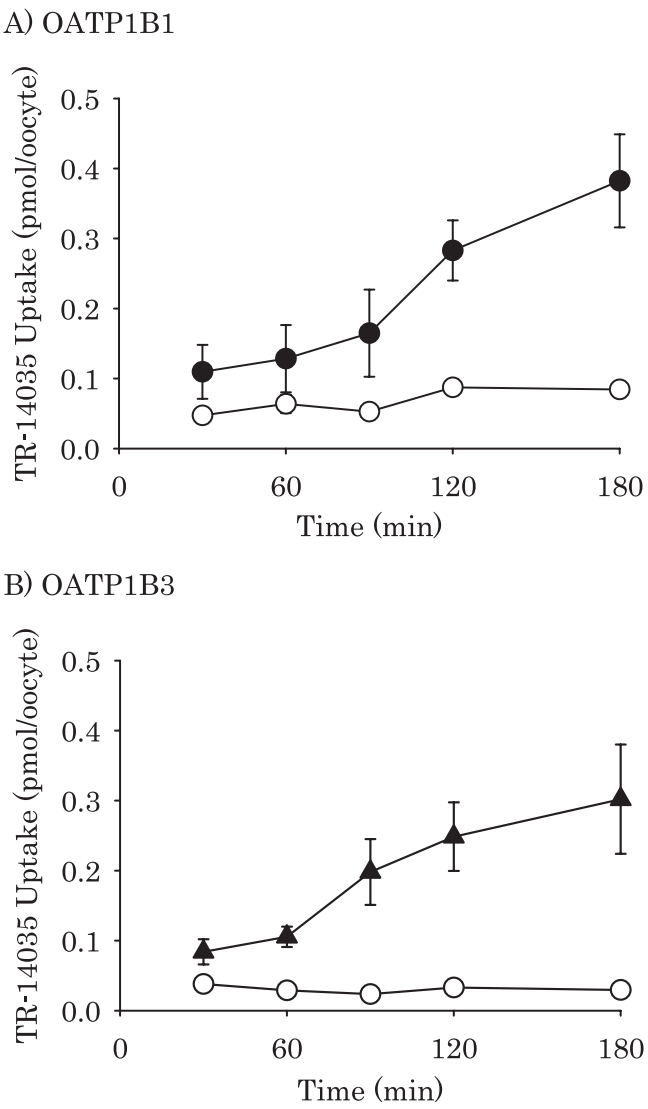

Fig. 5. Time course of TR-14035 uptake by uninjected: *open circles* (○) oocytes, and OATP1B1-: *closed circles* (●) and OATP1B3-: *closed triangles* (▲) expressing oocytes. Oocytes were incubated with 10 μM TR-14035 at room temperature for 30, 60, 90, 120 and 180 min. Each point represents the mean ± S.E. of eight to ten oocytes.

contrast, no effect of TEA, a typical substrate for OCTs, was observed on [^{14}C]TR-14035 uptake.

Uptake of TR-14035 by OATP-Expressing Oocytes

Time courses of TR-14035 uptake by human OATP1B1- and 1B3-expressing oocytes and uninjected control oocytes are shown in Fig. 5. Significant and time-dependent uptakes of TR-14035 were observed in OATP1B1- and 1B3-expressing oocytes compared with uninjected oocytes. Figure 6 shows the effect of substrate concentration on TR-14035 uptake by OATP-expressing and uninjected oocytes. The OATP1B1- and 1B3-mediated uptakes, obtained by subtracting the uptake velocity in uninjected oocytes from that in OATP-expressing oocytes, were increased in a concentration-dependent manner. The calculated kinetic parameters are summarized in Table II. The K_m values were 7.50 ± 0.52 and 5.28 ± 0.58 μM in OATP1B1 and 1B3 oocytes, respectively. Uptake activities of 10 μM TR-14035 in human OATP1A2- and 2B1-expressing oocytes and control oocytes were 1.25 ± 0.34, 0.077 ± 0.012 and 0.076 ± 0.009 pmol/oocyte/h, respectively. These results indicate that OATP1A2 is also capable to transport TR-14035, but OATP2B1 is not.

Uptake of TR-14035 by Stable OATP1B1*1a- and OATP1B1*15-Expressing Cells

Time courses of uptake of [^{3}H]estrone 3-sulfate, a typical substrate for OATP1B1, and TR-14035 by human OATP1B1*1a- and 1B1*15-expressing cells are shown in Fig. 7. Uptake of [^{3}H]estrone 3-sulfate by the cells expressed with

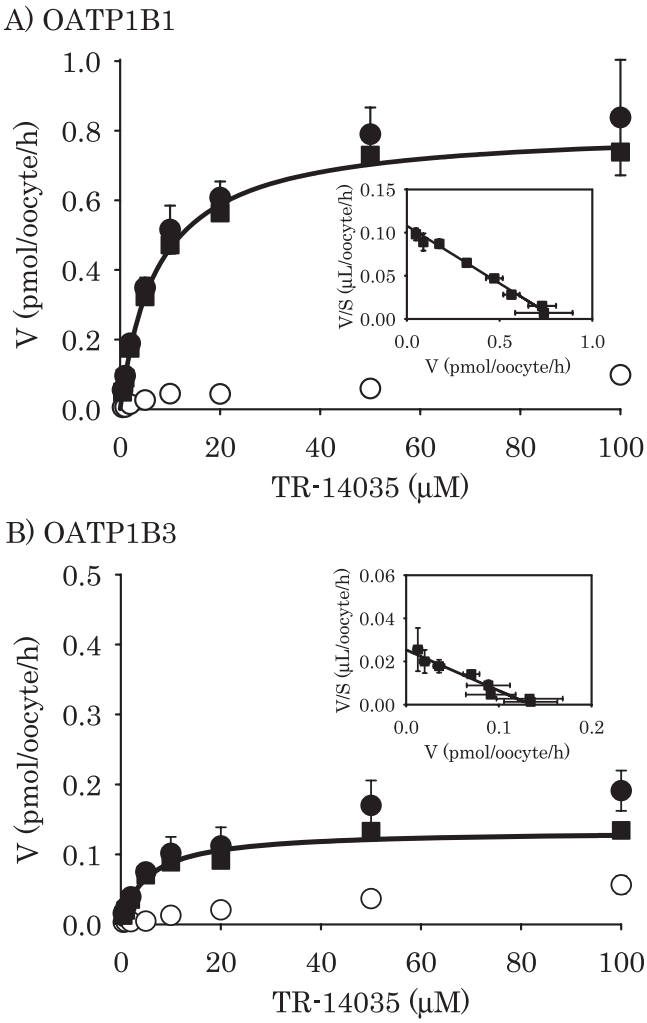

Fig. 6. Concentration-dependence of TR-14035 uptake by OATP1B1- (A) and OATP1B3- (B) expressing oocytes. Oocytes were incubated with TR-14035 at room temperature for 120 min. *Open* (○) and *closed* (●) *circles* represent uninjected and OATP cRNA injected oocytes, respectively. OATP-mediated uptake: *closed squares* (■) was obtained by subtracting the transport velocity in uninjected oocytes from that in OATP-expressing oocytes. *Solid lines* represent the fitted curves obtained by non-linear regression analysis. *Inset*, Eadie–Hofstee plot for the data. Each point represents the mean ± S.E. of eight to 11 oocytes.

Table II. Kinetic Parameters of TR-14035 Uptake in Human OATP1B1- and OATP1B3-Expressing Oocytes

OATP Isoforms	K_m	V_{max}
	(μM)	(pmol/oocyte/h)
OATP1B1	7.50 ± 0.52	0.809 ± 0.016
OATP1B3	5.28 ± 0.58	0.134 ± 0.008

Data shown in Fig. 6 were used to determine these parameters calculated by nonlinear regression analysis. Each value represents the mean ± S.D. of the parameter estimate generated by the MULTI program.

OATP1B1*1a or 1B1*15 was time-dependent and increased compared with that by mock cells. The uptake rates evaluated from the slopes of the curves of OATP1B1-mediated [^{3}H]estrone 3-sulfate uptake were 0.65 ± 0.05 and 0.32 ± 0.03 μl/mg protein/sec in OATP1B1*1a and 1B1*15 cells, respectively, signifying that the OATP1B1-mediated uptake in OATP1B1*15 cells was significantly reduced to the half of that in OATP1B1*1a cells.

Correspondingly, OATP1B1*1a and OATP1B1*15 cells provided increased uptakes of TR-14035 compared with mock cells, and the uptake rates evaluated from the slopes of the curves of OATP1B1-mediated TR-14035 uptake were 0.68 ± 0.03 and 0.32 ± 0.02 μl/mg protein/sec in OATP1B1*1a and 1B1*15 cells, respectively. This demonstrates that the OATP1B1-mediated TR-14035 uptake in OATP1B1*15 cells was decreased to the half of that in OATP1B1*1a cells.

Biliary Excretion of TR-14035 in EHBRs, *Mdr1a/b* KO and *Bcrp* KO Mice

Figure 8 shows the plasma concentrations and cumulative recoveries of unchanged TR-14035 in bile following intravenous administration to the bile duct-cannulated normal rats and EHBRs, and their estimated pharmacokinetic parameters are summarized in Table III. Plasma exposure of unchanged drug was significantly higher in EHBRs than in normal rats, indicating a lower CL_{tot} and longer MRT in EHBRs than in normal rats for TR-14035. In contrast, *Vd* and plasma protein binding in EHBRs were similar to those in normal rats. The cumulative biliary excretion of TR-14035 in EHBRs 4 h after administration (12.5 ± 2.2%) was much lower than that in normal rats (29.4 ± 4.1%). The CL_b of TR-14035 in EHBRs was significantly decreased to approximately 40% of that in normal rats. Conversely, the CL_r in EHBRs was increased 7.5-fold compared with normal rats.

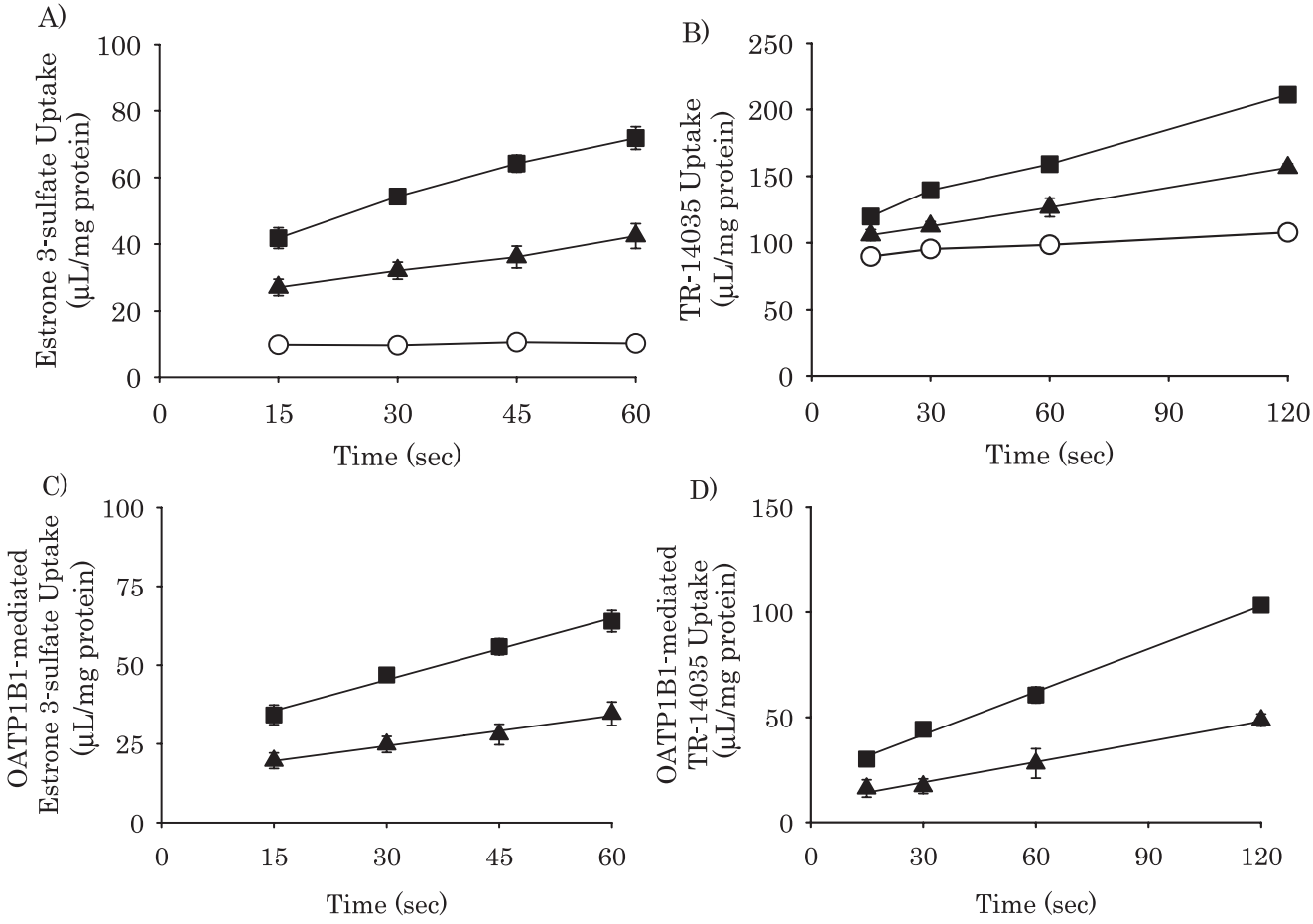

Fig. 7. Time course of [^{3}H]estrone 3-sulfate (A, C) and TR-14035 (B, D) uptake by Flp-In-293 cells stably transfected with OATP1B1*1a: *closed squares* (■), OATP1B1*15: *closed triangles* (▲) and mock: *open circles* (○). The cells were incubated with 8.7 nM [^{3}H]estrone 3-sulfate or 2.5 μM TR-14035 at 25°C for the desired time. OATP1B1-mediated uptake (C, D) was obtained by subtracting the uptake in mock from that in OATP1B1-expressing cells. *Solid lines* in (C) and (D) represent the fitted curves obtained by non-linear regression analysis. Each point represents the mean ± S.E. of four experiments.

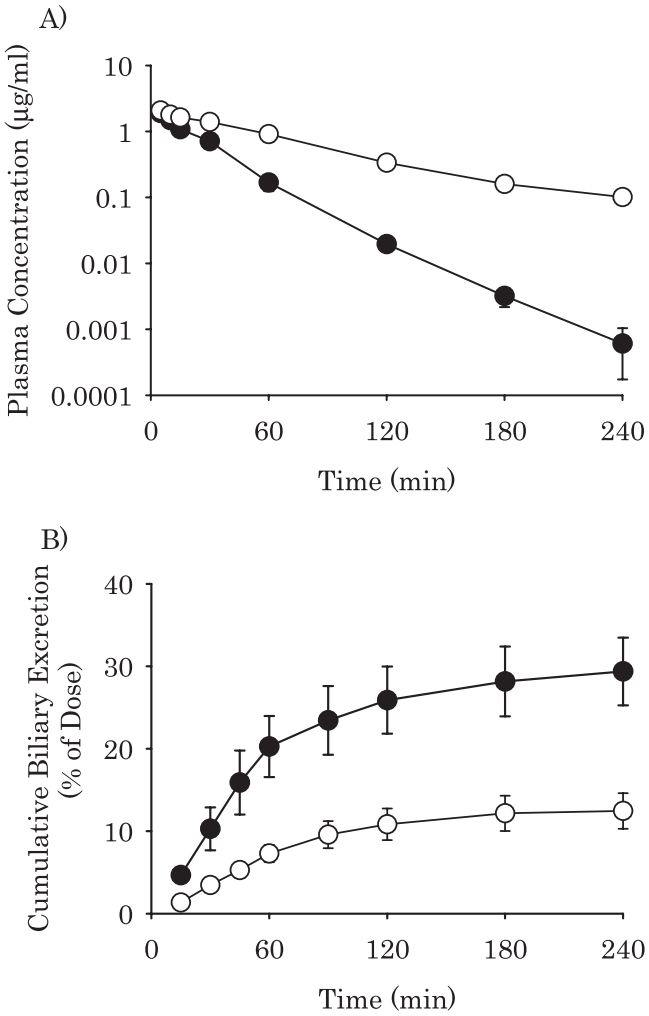

Fig. 8. Plasma concentrations (A) and cumulative biliary excretion (B) of TR-14035 after intravenous administration to normal rats (*closed circles* (●)) and EHBRs (*open circles* (○)) at a dose of 3 mg/kg. Each point represents the mean ± S.E. of four rats.

Plasma concentrations and cumulative recoveries of unchanged TR-14035 in bile following intravenous administration to the bile duct-cannulated wild (FVB), *mdr1a/b* KO and *Bcrp* KO mice are shown in Fig. 9. Plasma exposure and biliary excretion of TR-14035 in *mdr1a/b* or *Bcrp* KO mice were comparable to those in wild mice. Their corresponding pharmacokinetic parameters, presented in Table IV, showed overall similarity between wild and *mdr1a/b* or *Bcrp* KO mice.

DISCUSSION

In the present study, we investigated the hepatobiliary transport mechanisms of TR-14035 by performing *in vitro* uptake studies using hepatocytes, OATP-expressing oocytes and OATP-expressing Flp-In-293 cells, and *in vivo* biliary excretion studies using *mdr1a/b* KO, *Bcrp* KO mice and EHBRs. The results provide direct evidence that TR-14035 accumulates in the liver via transport proteins belonging to OATP family including polymorphic OATP1B1, and is mainly excreted into bile by Mrp2.

TR-14035 is moderately lipophilic ($\log D_{(pH\ 7.4)}$, 0.21), has an anionic moiety, and exhibits relatively high binding to plasma protein (Tables III and IV), which reflects the low distribution volume of TR-14035 in the rat (0.77 l/kg) and dog (0.52 l/kg) (4). However, the quantitative whole-body autoradiography in rats shows TR-14035 extremely and selectively accumulates in the liver shortly after intravenous and oral administration, in contrast to a much lower level in other tissues (data not shown). This result indicates that a carrier-mediated uptake system should mediate the specific accumulation of TR-14035 into the liver. Additionally, this hepatic uptake process is a first step in the clearance of TR-14035 from the body, because major elimination routes of TR-14035 are hepatic metabolism and biliary excretion. Hence, detailed investigations of hepatic uptake system of TR-14035 with further studies of biliary excretion system are critical for the understanding of TR-14035 pharmacokinetics in human as well as experimental animals.

In vitro uptake experiments in hepatocytes were performed to verify the mechanism of the hepatic uptake system of TR-14035. Figures 2 and 3 clearly indicate that TR-14035 accumulates in both rat and human hepatocytes in a time- and concentration-dependent manner. The apparent K_m values estimated are 6.33 μM in rat and 3.31 μM in human (Table I), and their transporter-mediated uptake clearances, calculated by V_{max}/K_m, are greater than their k_{ns} values. These initial uptakes were inhibited by ATP depletors and 200-times unlabeled TR-14035 (Fig. 4). These results suggest that TR-14035 mainly accumulates in hepatocytes by a transporter-mediated mechanism. To speculate what kind of transporters are responsible for the hepatic uptake, the uptake by hepatocytes was examined in the presence of typical inhibitors of hepatic drug transporters (Fig. 4). Significant inhibition by taurocholate, a typical substrate of OATPs and NTCP, and no effect of replacement of sodium with choline in the incubation medium suggest that sodium-independent OATPs are manly involved in hepatic uptake of TR-14035 in the rat and human, and sodium-dependent

Table III. Pharmacokinetic Parameters of Unchanged TR-14035 Following Intravenous Administration of TR-14035 at a Dose of 3 mg/kg to the Bile Duct-Cannulated Normal Rats and EHBRs

	AUC	CL_{tot}	MRT	Vd	CL_b	CL_r	PPB
	(μg min/ml)	(ml/min/kg)	(min)	(l/kg)	(ml/min/kg)	(ml/min/kg)	(%)
Normal	59.0 ± 5.8	52.2 ± 4.8	23.2 ± 2.4	1.18 ± 0.07	15.5 ± 2.9	0.132 ± 0.045	88.9 ± 0.2
EHBR	147 ± 17**	19.9 ± 2.1**	73.7 ± 4.7**	1.46 ± 0.18	2.72 ± 0.69*	0.991 ± 0.269*	90.4 ± 0.3

Each value represents the mean ± S.E. of four rats.
*Significantly different ($p < 0.05$) from normal rats.
**Significantly different ($p < 0.01$) from normal rats.

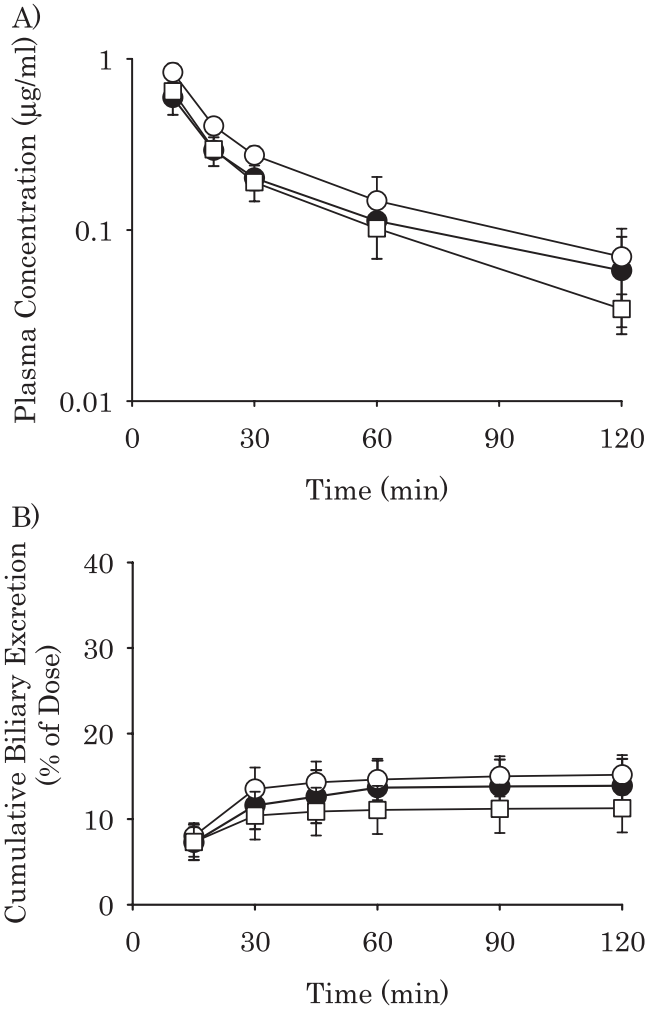

Fig. 9. Plasma concentrations (**A**) and cumulative biliary excretion (**B**) of TR-14035 after intravenous administration to wild: *closed circles* (●), *mdr1a/b* KO: *open circles* (○) and *Bcrp* KO mice: *open squares* (□) at a dose of 3 mg/kg. Each point represents the mean ± S.E. of four mice.

NTCP is not involved. Digoxin also inhibited the uptake in both hepatocytes, which indicates Oatp1a4 in rat and OATP1B3 in human may be involved in the TR-14035 accumulation in hepatocytes. PAH, a typical substrate of the OAT family, partially reduced the uptake in rat but not in human, indicating OAT may be, in part, responsible for the uptake by rat hepatocytes. In contrast, TEA, a typical substrate of the OCT family, had no effect on the hepatic uptake, suggesting the OCT family is not concerned with hepatic uptake of TR-14035. These results indicate that transporters belonging to the OATP family might be principally involved in the accumulation in hepatocytes.

In order to directly determine the potential of OATPs for transport of TR-14035, we examined the transport of TR-14035 by human OATP1B1 and OATP1B3, main isoforms expressed at the sinusoidal membrane in human hepatocytes, using a *X. laevis* oocyte expressing system. Time- and concentration-dependent uptakes of TR-14035 were observed in OATP1B1 and OATP1B3 oocytes (Figs. 5 and 6). The K_m values were 7.50 and 5.28 μM, respectively (Table II), similar to that of uptake by human hepatocytes. These results suggest that both OATP1B1 and 1B3 are responsible for the transport in human hepatocytes. However, in the uptake experiment by human hepatocytes, Eadie-Hofstee plot gave apparently one saturable component, indicating that single transporter should mediate the uptake. This apparent inconsistent observation may be due to the similarity of the K_m values for OATP1B1 and 1B3 and/or single isoform should predominantly mediate the hepatic uptake. Additionally, OATP1A2 also exhibited a predominant transport activity of TR-14035, but OATP2B1 did not, in the present study. However, because OATP1A2 expression was localized specifically to cholangiocytes but not to hepatocytes (18), OATP1B1 and 1B3 should be involved in the uptake by hepatocytes.

Pharmacokinetics and biliary excretion experiments using *Mrp2*-deficiant EHBRs and *mdr1a/b* KO and *Bcrp* KO mice were performed to identify the transporters mediating the biliary excretion of TR-14035. The present study showed that only approximately 12% of the intravenously administered dose was excreted into bile of *Mrp2*-deficient EHBRs as unchanged TR-14035, though approximately 30% of the dose was excreted in normal rat bile, indicating CL_b in EHBR was significantly decreased compared to that in normal rat (Fig. 8 and Table III). On the other hand, the clearances in *mdr1a/b* KO and *Bcrp* KO mice were overall similar to wild (FVB) mice (Fig. 9 and Table IV). These results suggest that Mrp2 is one of the principal transport proteins responsible for the biliary excretion of unchanged TR-14035, and mdr1a/b and Bcrp contribute little to this excretion. Incomplete disappearance of biliary excretion of TR-14035 in EHBR also suggests that a further unknown transport system, other than mdr1a/b, Bcrp and Mrp2, might mediate the biliary excretion. Recently, it has been reported that bile salt export pump can transport a nonbile acid, pravastatin, which is a well-known 3-hydroxy-3-methylglutaryl-CoA reductase inhibitor (19). This transporter may be partly involved in the biliary excretion of TR-14035.

Table IV. Pharmacokinetic Parameters of Unchanged TR-14035 Following Intravenous Administration of TR-14035 at a Dose of 3 mg/kg to the Bile Duct-Cannulated Wild, *mdr1a/b* KO and *Bcrp* KO Mice

	AUC	CL_{tot}	MRT	*Vd*	CL_b	PPB
	(μg min/ml)	(ml/min/kg)	(min)	(l/kg)	(ml/min/kg)	(%)
Wild	24.6 ± 6.6	131 ± 30	49.8 ± 14.6	5.43 ± 0.85	18.0 ± 2.9	87.6 ± 0.1
mdr1a/b KO	33.5 ± 6.0	88.4 ± 16.8	47.1 ± 13.5	3.58 ± 0.39	15.8 ± 4.6	88.1 ± 0.4
Bcrp KO	24.7 ± 1.1	114 ± 5	35.9 ± 5.6	4.08 ± 0.62	14.0 ± 3.8	86.8 ± 0.5

Each value represents the mean ± S.E. of four mice.
All data in KO mice were not significantly different from wild mice.

In our previous investigation, TR-14035 was principally metabolized by polymorphic human CYP2C9 and the variant CYP2C9*3 was associated with a reduced metabolic clearance of TR-14035 *in vitro* (5), indicating that clinical pharmacokinetic profile of TR-14035 should be affected by *CYP2C9* genotype. The present study indicates that OATP1B1 should at least partly mediate the hepatic uptake of TR-14035 in human. It is known that *OATP1B1* is polymorphic and ethnic difference of its variants have been reported (20,21). Among OATP1B1 variants, OATP1B1*15 exhibits decreased transport activities of substrates *in vitro* (22–24) and increased plasma exposures of its substrates in human *in vivo* (25–27). To determine the effect of this SNP on the transport of TR-14035, we compared the transport activities between OATP1B1*1a and OATP1B1*15, since OATP1B1*15 was suggested to cause significant reduction of its transport activity (24). A decreased transport of TR-14035 in the cells stably transfected with OATP1B1*15 was observed compared with that in the cells transfected with OATP1B1*1a (Fig. 7). mRNA expression levels between OATP1B1*1a and *15 transfectants were similar (data not shown). Their transcriptional activities and mRNA stabilities should be generally comparable. Iwai *et al*. (22) and Kameyama *et al*. (28) have reported that V_{max} normalized by protein level for OATP1B1*15 was significantly decreased compared with OATP1B1*1a, but K_m was not. Therefore, a decreased transport activity of TR-14035 in OATP1B1*15 transfectant should be due to a decreased V_{max} of this variant. This result, together with the fact that not only OATP1B1 but also OATP1B3 mediate TR-14035 transport, indicates that TR-14035 should be also affected by *OATP1B1* genotype, and effect of the genotype should vary by the relative contribution of OATP1B1 to the overall hepatic uptake of TR-14035. A clinical evaluation should be necessary for identification of the effect of SNPs. A recent report showed that the pharmacokinetics of repaglinide, a meglitinide analog antidiabetic drug, is associated with SNPs of both the *OATP1B1* and *CYP2C8* genes (29). Therefore, we should pay attention to the potential for interindividual variability in the pharmacokinetics of TR-14035 due to SNPs in both *OATP1B1* and *CYP2C9* genes.

Recently, clinically relevant drug–drug interactions based on OATP-mediated transport in the liver have been reported (30). For example, concomitant administration of rosuvastatin with cyclosporin A, a potent OATP inhibitor (IC_{50} on rosuvastatin uptake, 2.2 μM), resulted in a clinically significant, 11-fold increase in maximum plasma concentration and sevenfold increase in AUC for rosuvastatin (31). Gemfibrozil, also a potent OATP inhibitor (IC_{50} on rosuvastatin uptake, 4.0 μM), when co-administered with rosuvastatin, gave 2.2- and 1.9-fold increases in maximum plasma concentration and AUC, respectively, for rosuvastatin (32). The K_m values of TR-14035 determined by the uptake experiment using hepatocytes and OATP-expressing oocytes were less than 10 μM in the current study (Tables I and II). Therefore, inhibition of OATP1B1 and 1B3 by TR-14035 may result in a reduced hepatic uptake clearance of co-administered OATP substrate, and the subsequent increase of the exposure may occur in the clinic.

In vitro O-desmethylation clearances of TR-14035 in rat and human liver microsomes were low, 35 and 20 μl/min/mg protein, respectively (4), and the protein bindings to rat and human plasma were high, 89 and 99%, respectively (Table III; unpublished data), predicting that TR-14035 should be conventionally judged to be metabolically stable in the rat and human. However, the exposure of the *O*-desmethyl derivative was evidently high compared with unchanged drug in the rat and human (4, unpublished data). This greatly enhanced *in vivo* metabolism may be due to an OATP-mediated accumulation in liver. Recently, it has been reported that the interplay between drug transporters and enzymes should be considered in evaluating drug disposition (33–35), which supports the proposed mechanism of indirect acceleration of TR-14035 metabolism by OATP1B1 and 1B3.

In conclusion, TR-14035 accumulates in the liver via a carrier-mediated transport system including OATP1B1 and 1B3 with high affinities, and is excreted into bile predominantly by Mrp2. Furthermore, genetic polymorphisms of *OATP1B1* may cause an interindividual variability in the pharmacokinetics of TR-14035.

ACKNOWLEDGMENTS

We thank Yoko Togo, Masao Yamanouchi, Kyoko Ozawa and Masakatsu Takahashi for their expert technical assistance in biliary excretion studies.

REFERENCES

1. C. Berlin, E. L. Berg, M. J. Briskin, D. P. Andrew, P. J. Kilshaw, B. Holzmann, I. L. Weissman, A. Hamann, and E. C. Butcher. α4β7 integrin mediates lymphocyte binding to the mucosal vascular addressin MAdCAM-1. *Cell* **74**:185–195 (1993).
2. C. Berlin, R. F. Bargatze, J. J. Campbell, U. H. von Andrian, M. C. Szabo, S. R. Hasslen, R. D. Nelson, E. L. Berg, S. L. Erlandsen, and E. C. Butcher. α4 integrins mediate lymphocyte attachment and rolling under physiologic flow. *Cell* **80**:413–422 (1995).
3. I. Sircar, K. S. Gudmundsson, R. Martin, J. Liang, S. Nomura, H. Jayakumar, B. R. Teegarden, D. M. Nowlin, P. M. Cardarelli, J. R. Mah, S. Connell, R. C. Griffith, and E. Lazarides. Synthesis and SAR of *N*-benzoyl-L-biphenylalanine derivatives: discovery of TR-14035, a dual α4β7/α4β1 integrin antagonist. *Bioorg. Med. Chem.* **10**:2051–2066 (2002).
4. M. Tsuda-Tsukimoto, Y. Ogasawara, and T. Kume. Pharmacokinetics and metabolism of TR-14035, a novel antagonist of α4β1/α4β7 integrin mediated cell adhesion, in rat and dog. *Xenobiotica* **35**:373–389 (2005).
5. M. Tsuda-Tsukimoto, Y. Ogasawara, and T. Kume. Role of human liver cytochrome *P*450 2C9 in the metabolism of a novel α4β1/α4β7 dual antagonist, TR-14035. *Drug Metab. Pharmacokinet.* **20**:127–134 (2005).
6. B. Hagenbuch and P. J. Meier. Organic anion transporting polypeptides of the OATP/SLC21 family: phylogenetic classification as OATP/SLCO superfamily, new nomenclature and molecular/functional properties. *Pflugers Arch.* **447**:653–665 (2004).
7. H. Koepsell and H. Endou. The SLC22 drug transporter family. *Pflugers Arch.* **447**:666–676 (2004).
8. P. Chandra and K. L. Brouwer. The complexities of hepatic drug transport: current knowledge and emerging concepts. *Pharm. Res.* **21**:719–735 (2004).
9. B. Sarkadi, C. Özvegy-Laczka, K. Német, and A. Váradi. ABCG2—a transporter for all seasons. *FEBS Lett.* **567**:116–120 (2004).
10. H. Baur, S. Kasperek, and E. Pfaff. Criteria of viability of

isolated liver cells. *Hoppe-Seyler Z. Physiol. Chem.* **356**:827–838 (1975).
11. Y. Shitara, T. Itoh, H. Sato, A. P. Li, and Y. Sugiyama. Inhibition of transporter-mediated hepatic uptake as a mechanism for drug–drug interaction between cerivastatin and cyclosporin A. *J. Pharmacol. Exp. Ther.* **304**:610–616 (2003).
12. M. Schwenk. Transport systems of isolated hepatocytes: studies on the transport of biliary compounds. *Arch. Toxicol.* **44**:113–126 (1980).
13. I. Tamai, T. Nozawa, M. Koshida, J. Nezu, Y. Sai, and A. Tsuji. Functional characterization of human organic anion transporting polypeptide B (OATP-B) in comparison with liver-specific OATP-C. *Pharm. Res.* **18**:1262–1269 (2001).
14. M. Tsuda, T. Sekine, M. Takeda, S. H. Cha, Y. Kanai, M. Kimura, and H. Endou. Transport of ochratoxin A by renal multispecific organic anion transporter 1. *J. Pharmacol. Exp. Ther.* **289**:1301–1305 (1999).
15. M. Jordan, A. Schallhorn, and F. M. Wurm. Transfecting mammalian cells: optimization of critical parameters affecting calcium–phosphate precipitate formation. *Nucleic Acids Res.* **24**:596–601 (1996).
16. I. Tamai, J. Nezu, H. Uchino, Y. Sai, A. Oku, M. Shimane, and A. Tsuji. Molecular identification and characterization of novel members of the human organic anion transporter (OATP) family. *Biochem. Biophys. Res. Commun.* **273**:251–260 (2000).
17. K. Yamaoka, Y. Tanigawara, T. Nakagawa, and T. Uno. A pharmacokinetics analysis program (MULTI) for microcomputer. *J. Pharmacobio-Dyn.* **4**:879–885 (1981).
18. W. Lee, H. Glaeser, L. H. Smith, R. L. Roberts, G. W. Moeckel, G. Gervasini, B. F. Leake, and R. B. Kim. Polymorphisms in human organic anion-transporting polypeptide 1A2 (OATP1A2): implications for altered drug disposition and central nervous system drug entry. *J. Biol. Chem.* **280**:9610–9617 (2005).
19. M. Hirano, K. Maeda, H. Hayashi, H. Kusuhara, and Y. Sugiyama. Bile salt export pump (BSEP/ABCB11) can transport a nonbile acid substrate, pravastatin. *J. Pharmacol. Exp. Ther.* **314**:876–882 (2005).
20. R. G. Tirona, B. F. Leake, G. Merino, and R. B. Kim. Polymorphisms in OATP-C: identification of multiple allelic variants associated with altered transport activity among European- and African-Americans. *J. Biol. Chem.* **276**:35669–35675 (2001).
21. T. Nozawa, M. Nakajima, I. Tamai, K. Noda, J. Nezu, Y. Sai, A. Tsuji, and T. Yokoi. Genetic polymorphisms of human organic anion transporters OATP-C (SLC21A6) and OATP-B (SLC21A9): allele frequencies in the Japanese population and functional analysis. *J. Pharmacol. Exp. Ther.* **302**:804–813 (2002).
22. M. Iwai, H. Suzuki, I. Ieiri, K. Otsubo, and Y. Sugiyama. Functional analysis of single nucleotide polymorphisms of hepatic organic anion transporter OATP1B1 (OATP-C). *Pharmacogenetics* **14**:749–757 (2004).
23. T. Nozawa, S. Sugiura, M. Nakajima, A. Goto, T. Yokoi, J. Nezu, A. Tsuji, and I. Tamai. Involvement of organic anion transporting polypeptides in the transport of troglitazone sulfate: implications for understanding troglitazone hepatotoxicity. *Drug Metab. Dispos.* **32**:291–294 (2004).
24. T. Nozawa, H. Minami, S. Sugiura, A. Tsuji, and I. Tamai. Role of organic anion transporter OATP1B1 (OATP-C) in hepatic uptake of irinotecan and its active metabolite, 7-ethyl-10-hydroxycamptothecin: *in vitro* evidence and effect of single nucleotide polymorphisms. *Drug Metab. Dispos.* **33**:434–439 (2005).
25. Y. Nishizato, I. Ieiri, H. Suzuki, M. Kimura, K. Kawabata, T. Hirota, H. Takane, S. Irie, H. Kusuhara, Y. Urasaki, A. Urae, S. Higuchi, K. Otsubo, and Y. Sugiyama. Polymorphisms of OATP-C (SLC21A6) and OAT3 (SLC22A8) genes: consequences for pravastatin pharmacokinetics. *Clin. Pharmacol. Ther.* **73**:554–565 (2003).
26. M. Niemi, E. Schaeffeler, T. Lang, M. F. Fromm, M. Neuvonen, C. Kyrklund, J. T. Backman, R. Kerb, M. Schwab, P. J. Neuvonen, M. Eichelbaum, and K. T. Kivistö. High plasma pravastatin concentrations are associated with single nucleotide polymorphisms and haplotypes of organic anion transporting polypeptide-C (OATP-C, SLCO1B1). *Pharmacogenetics* **14**:429–440 (2004).
27. M. Niemi, K. T. Kivistö, U. Hofmann, M. Schwab, M. Eichelbaum, and M. F. Fromm. Fexofenadine pharmacokinetics are associated with a polymorphism of the *SLCO1B1* gene (encoding OATP1B1). *Br. J. Clin. Pharmacol.* **59**:602–604 (2005).
28. Y. Kameyama, K. Yamashita, K. Kobayashi, M. Hosokawa, and K. Chiba. Functional characterization of SLCO1B1 (OATP-C) variants, SLCO1B1*5, SLCO1B1*15 and SLCO1B1*15 + C1007G, by using transient expression systems of HeLa and HEK293 cells. *Pharmacogenet. Genomics* **15**:513–522 (2005).
29. M. Niemi, J. T. Backman, L. I. Kajosaari, J. B. Leathart, M. Neuvonen, A. K. Daly, M. Eichelbaum, K. T. Kivistö, and P. J. Neuvonen. Polymorphic organic anion transporting polypeptide 1B1 is a major determinant of repaglinide pharmacokinetics. *Clin. Pharmacol. Ther.* **77**:468–478 (2005).
30. Y. Shitara, H. Sato, and Y. Sugiyama. Evaluation of drug–drug interaction in the hepatobiliary and renal transport of drugs. *Annu. Rev. Pharmacol. Toxicol.* **45**:689–723 (2005).
31. S. G. Simonson, A. Raza, P. D. Martin, P. D. Mitchell, J. A. Jarcho, C. D. Brown, A. S. Windass, and D. W. Schneck. Rosuvastatin pharmacokinetics in heart transplant recipients administered an antirejection regimen including cyclosporine. *Clin. Pharmacol. Ther.* **76**:167–177 (2004).
32. D. W. Schneck, B. K. Birmingham, J. A. Zalikowski, P. D. Mitchell, Y. Wang, P. D. Martin, K. C. Lasseter, C. D. Brown, A. S. Windass, and A. Raza. The effect of gemfibrozil on the pharmacokinetics of rosuvastatin. *Clin. Pharmacol. Ther.* **75**:455–463 (2004).
33. C. -Y. Wu and L. Z. Benet. Disposition of tacrolimus in isolated perfused rat liver: influence of troleandomycin, cyclosporine and GG918. *Drug Metab. Dispos.* **31**:1292–1295 (2003).
34. Y. Y. Lau, C. -Y. Wu, H. Okochi, and L. Z. Benet. Ex situ inhibition of hepatic uptake and efflux significantly changes metabolism: hepatic enzyme-transporter interplay. *J. Pharmacol. Exp. Ther.* **308**:1040–1045 (2004).
35. L. Liu and K. S. Pang. The roles of transporters and enzymes in hepatic drug processing. *Drug Metab. Dispos.* **33**:1–9 (2005).